Limnol. Oceanogr., 50(5), 2005, 1499–1510

Parameterizing the natural fluorescence kinetics of *Thalassiosira weissflogii*

S. R. Laney,[1] *R. M. Letelier, and M. R. Abbott*
College of Oceanic & Atmospheric Sciences, Oregon State University, Corvallis, Oregon 97331-5503

Abstract

We examined variability in the natural fluorescence yield of a neritic diatom, *Thalassiosira weissflogii*, in continuous cultures. In this species, kinetics in natural fluorescence yield over time scales less than a photoperiod were characterized by sharp decreases, occurring at irradiance intensities that presumably coincide with the onset of nonphotochemical fluorescence quenching by interconvertible xanthophylls. The irradiance at which these decreases occurred, and the concomitant degree of quenching involved, varied systematically in these cultures as a function of dilution rate and irradiance intensity, independent of biomass. Similar diurnal kinetics in natural fluorescence yield were observed in phytoplankton assemblages in a coastal transition region in the Gulf of Alaska. An empirical parameterization was developed to quantify these diurnal kinetics in terms of the magnitude of this increased quenching and the irradiance at which it occurred, in order to track the behavior of these kinetics over longer time scales of days to weeks.

During daytime, phytoplankton assemblages in the surface ocean emit low but detectable levels of chlorophyll fluorescence around 683 nm. This emission is referred to as natural fluorescence, F_{nat}, or often as passive, sun-stimulated or solar fluorescence. It can be measured in situ using radiometers mounted on profilers or drifters, and its water-leaving component can be detected from ships, aircraft, or satellites (Gower and Borstad 1981; Kiefer et al. 1989; Letelier and Abbott 1996). Satellite radiometers with channels in the natural fluorescence wavelengths, like the Moderate Resolution Imaging Spectroradiometer (MODIS) and the Medium Resolution Imaging Spectrometer (MERIS), currently measure surface ocean F_{nat} over wide spatial and temporal scales.

Several studies have indicated a broad correlation between the chlorophyll biomass of oceanic phytoplankton assemblages and either F_{nat} or the ratio of F_{nat} to ambient irradiance (i.e., the F_{nat} yield) (Neville and Gower 1977; Borstad et al. 1985; Kiefer et al. 1989). As a result, algorithms have been developed to estimate surface ocean chlorophyll from remotely sensed F_{nat} (IOCCG 1999; Hoge et al. 2003). Such algorithms may be particularly useful in Case II waters, where the presence of nonphytoplankton scatterers and absorbers degrades the standard radiance reflectance algorithms for chlorophyll. An examination of MODIS natural fluorescence in Oregon coastal waters indicates that F_{nat}-based estimates of chlorophyll are less sensitive to these factors and to the aerosol correction model used (Letelier unpubl. data).

Remotely sensed F_{nat} data may potentially provide new insights into global and seasonal patterns in ocean productivity (Esaias et al. 1998; IOCCG 1999). Studies that have examined the relationship between F_{nat} and different aspects of primary production and photosynthesis (e.g., Kiefer et al. 1989; Stegmann et al. 1992; Garcia-Mendoza and Maske 1996) have failed to identify a robust relationship between F_{nat} and phytoplankton growth. The lack of a simple relationship between F_{nat} yield and photosynthetic processes in phytoplankton reflects the complexity of light absorption and fluorescence in vivo. Several photosynthetic responses can considerably alter the F_{nat} yield of phytoplankton, and responses such as nonphotochemical quenching are particularly relevant to remote sensing of F_{nat} because they occur in the well-lit top optical depths that contribute the majority of water-leaving F_{nat} (Cullen and Lewis 1995).

Although F_{nat} yield is affected by complex physiological processes, its variability in natural phytoplankton assemblages is not random. Systematic changes in F_{nat} yield are often observed in association with physical features like upwelling eddies (Letelier et al. 1997, 2000), frontal circulation features (Abbott et al. 2000), and meandering jets (Abbott et al. 2001). These observations indicate that natural fluorescence kinetics under these conditions reflect broad physiological responses to environmental perturbation. However, describing these kinetics in terms of specific photosynthetic responses has been difficult. A major challenge facing marine ecologists is the development of analytical methods that provide ecologically meaningful interpretations of variability in remotely sensed F_{nat}.

Models for natural fluorescence variability

Variability in F_{nat} has often been interpreted using simple spectroscopic models, originally developed to describe the fluorescence of inert fluorophores in solution. These models have been only partly successful in relating variability in phytoplankton F_{nat} to specific physiological or ecological properties like chlorophyll biomass or photosynthetic state.

[1] Corresponding author (slaney@coas.oregonstate.edu).

Acknowledgments

We thank Dale Kiefer for the prototype instrument we modified for these experiments and John Morrow for background on its initial use. Claudia Mengelt and Lisa Eisner assisted in the laboratory, and Curt Vandetta provided valuable computer support. We also thank Dave Musgrave and Scott Pegau for radiometer deployments during the 2003 GLOBEC-NEP Gulf of Alaska mesoscale cruises. Comments and suggestions from Ron Zaneveld, Russ Desiderio, Yannick Huot, Pat Wheeler, and two anonymous reviewers helped improve this manuscript considerably. This research was supported by the National Aeronautics and Space Administration (NAS5-31360 to M.R.A, NNG04HZ35C to R.M.L. and M.R.A., and NAS7-969 to Biospherical Instruments for the initial development of the chemostat apparatus).

Assumptions and approximations used to derive these spectroscopic models might be inappropriate or potentially misleading when such models are applied to living photosynthetic organisms, because there are subtle differences between how molecular solutions and phytoplankton suspensions fluoresce. We first review these models to evaluate how some of these assumptions and approximations may affect the interpretation of observed variability in F_{nat}.

The most basic expression for natural fluorescence involves three parameters: irradiance, E; absorptance, A; and the fluorescence quantum yield, ϕ^F. Absorptance is the fraction of ambient photons absorbed by the fluorescing substance, and the quantum yield represents the fraction of absorbed photons that are reemitted as fluorescence (Harris and Bertolucci 1978; Skoog et al. 1988). Assuming that E and F_{nat} are expressed in units of quanta, and neglecting their wavelength dependence, F_{nat} can be expressed as

$$F_{nat} = E \times A \times \phi^F \quad (1)$$

where both A and ϕ^F are dimensionless. In optically dilute solutions, A can be approximated by the product of fluorophore concentration and an empirically determined molar absorption coefficient. Absorptance in phytoplankton suspensions is often treated similarly, by defining a chlorophyll-specific absorption coefficient a^*. This leads to a relationship between the natural fluorescence yield (F_{nat}/E_{PAR}, for PAR irradiance in situ) and chlorophyll concentration *chl*.

$$F_{nat}/E_{PAR} = a^* \times chl \times \phi^F \quad (2)$$

Other expressions for F_{nat} found in the literature (e.g., Stegmann et al. 1992; Babin et al. 1996; Morrison 2003) may differ from Eq. 2 slightly because of unit or geometrical conversions, inclusion of a spectral dimension, or use of derived parameters, such as the total absorbed photon flux $A_{ex} \equiv E \times A$ (sensu Maritorena et al. 2000).

Models expressed by Eq. 2, and their more complex derivatives, seem to indicate that changes in chlorophyll biomass causally determine F_{nat} yield. From a physiological perspective, however, this cannot be strictly true because total *chl* is partitioned between the weakly fluorescent Photosystem I (PSI) and the strongly fluorescent Photosystem II (PSII). Changes in photosystem stoichiometry can affect F_{nat} yield independently of *chl* or absorption, but the degree to which this occurs in natural populations is not well understood. It is tempting to argue that ϕ^F effectively maintains causality between *chl* and F_{nat} by accounting for photosystem stoichiometry, but PSI and PSII have widely different pigment complements and, therefore, different chlorophyll-normalized absorptions. Like many other photosynthetic responses, it is difficult to assign changes in photosystem stoichiometry solely to either ϕ^F or a^*. Other responses that similarly decouple variability in F_{nat} from that of *chl* include state transitions, which alter the distribution of absorbed light energy between PSI and PSII. State transitions play an essential role in the photosynthetic ecology of cyanobacteria (Campbell et al. 1998; Sarcina et al. 2001), important photosynthetic prokaryotes in oligotrophic regions. Because ϕ^F and a^* are empirical parameters, they indicate only phenomenological changes in the F_{nat} versus irradiance relationship, not specific physiological or ecological responses per se. Furthermore, changes in ϕ^F or a^* may reflect different physiological processes in prokaryotes and eukaryotes (MacIntyre et al. 2002), which complicates interpreting these parameters in terms of specific photosynthetic responses.

Temporal scales of variability in natural fluorescence yield—Because Eq. 2 indicates only a correlation between F_{nat} yield and *chl*, and not a causal relationship per se, some researchers have suggested that F_{nat} yield cannot be used to examine both *chl* biomass and photosynthetic state (sensu Morrison 2003). To utilize F_{nat} yield as a proxy for *chl*, variability in ϕ^F and a^* must be negligible, and vice versa. Yet an important and often overlooked fact is that variability in F_{nat} yield occurs across a wide range of temporal scales. The diurnal photoperiod provides the natural time scale for separating the influence of *chl* biomass on F_{nat} yield from that of other photosynthetic factors. On scales longer than a photoperiod, changes in F_{nat} yield reflect photosynthetic adaptations in populations or changes in assemblage structure. On scales shorter than a photoperiod, changes in F_{nat} yield primarily result from short-term photosynthetic acclimations that affect photochemical and nonphotochemical fluorescence quenching. Changes in pigmentation affect F_{nat} yield to a much lesser extent over these short scales, and so F_{nat} variability on time scales below a photoperiod reflects photosynthetic responses that are largely independent of *chl* biomass.

Variability in F_{nat} may provide more detailed insight into the photosynthetic state of phytoplankton assemblages than the simplistic models described by Eq. 2, but scales of variability in F_{nat} have received little prior attention. Culture experiments can be valuable tools for exploring and characterizing F_{nat} variability in phytoplankton, because under controlled conditions it may be easier to determine the physiological bases for specific F_{nat} kinetics or to examine how these kinetics respond to changes in individual environmental properties. The need for such information is well acknowledged (e.g., Cullen and Lewis 1995; Falkowski and Kolber 1995; Cullen et al. 1997), but few laboratory studies of F_{nat} variability have been performed to date.

We used continuous cultures to examine how F_{nat} yield varied in the model neritic diatom *Thalassiosira weissflogii* (Bacillariophyceae) over subdiurnal to multigenerational scales and under different conditions of nitrate availability and irradiance intensity. Irradiance and nitrate availability represent two key environmental factors controlling F_{nat} yield, particularly in the upper portion of the water column that is remotely sensed (Chekalyuk and Gorbunov 1994). We concurrently monitored several other photosynthetic properties in these cultures, including PSII parameters, using variable fluorescence techniques and cell-specific concentrations of *chl* and major accessory pigments. Because of the large interest in remote sensing applications of F_{nat}, we focused on those kinetics that may be expected from phytoplankton living in high-irradiance conditions typical of the near-surface ocean.

Methods

Phytoplankton cultures—The system we designed to monitor F_{nat} kinetics in phytoplankton continuous cultures is pre-

sented in detail in Laney et al. (2001). We incubated two 1.5-liter cultures of the marine diatom *T. weissflogii* (Bacillariophyceae, strain CCMP 1051) under different irradiance and nitrate regimes. Growth rates of these continuous cultures were set by varying the dilution rate of an IMR medium in which phosphate and silicate were amended to IMR/2 (17.5 and 75 μmol L^{-1}, respectively) and nitrate to IMR/20 (25 μmol L^{-1}). To avoid carbon-limited growth during high-irradiance periods, culture pH was continuously monitored and kept below 8.2 by automatic metered addition of carbon dioxide–enriched air (2% CO_2). Cultures were continuously stirred and bubbled with 0.2-μm–filtered air, and culture temperature was maintained at 20°C ± 0.1°C.

Dilution rates and irradiance were manipulated to represent extremes on a spectrum of possible dilution rates and thus the range of nitrate-limited growth expected in nature. Dilution was slow but continuous throughout the entire 60 d of the first culture (0.11 d^{-1}), which we refer to as the ''constant'' dilution rate culture (CDR, Fig. 1a–d). Dilution rate in the second culture was manipulated such that no dilution occurred for the first 8 d after inoculation, followed by dilution at 0.74 d^{-1} for 21 d, and finally no dilution again for the final 11 d. The second culture thus experienced ''variable'' dilution rates (VDR, Fig. 1e–h), simulating, for example, an extended nutrient pulse.

Irradiance intensity in both cultures was computer controlled as a semisinusoid with a light–dark cycle of 14 : 10 h. Colored glass filters selected for a broadband blue–green spectrum of growth irradiance. In both the CDR and VDR cultures, the maximum photoperiod irradiance (E_{max}) was initially set to ≈80 μmol quanta m^{-2} s^{-1} (Fig. 1a,e). After waiting approximately five volume turnovers in the CDR experiment, E_{max} was increased to ≈400 μmol quanta m^{-2} s^{-1} (CDR day 48). In the VDR culture E_{max} was similarly increased on VDR day 21 after nine volume turnovers, during a period of rapid population growth resulting from a prior increase in dilution rate on VDR day 9. These different irradiance levels are referred to as the ''low'' and ''high'' E_{max} treatments.

On CDR days 14 and 29, during its initial stabilization period, a dilute erythromycin solution was added to determine its efficacy in controlling heterotrophic bacterial populations. The solution did not fluoresce and was not intended as a deliberate manipulation, but since these additions coincided with weak and temporary changes in the F_{nat} of the CDR culture, we note their influence (*see Results*).

Discrete culture assays—Both cultures were sampled once daily in the hour preceding the light period for cell abundance and pigment biomass. Abundance was determined using a Coulter Counter ZBI (Coulter), size-calibrated using microspheres. Concentrations and distributions of phytoplankton pigments were determined using high-pressure liquid chromatography (HPLC, detector: Thermo Separation Products UV2000, pump: Perkin Elmer 400) following Wright et al. (1997). The system was calibrated for chlorophyll *a* concentration and for the elution times of chlorophyll c_1 and c_2, β-carotene, fucoxanthin, diatoxanthin, and diadinoxanthin. Chlorophyll *a* concentrations were also determined using standard fluorometric methods (Turner Designs

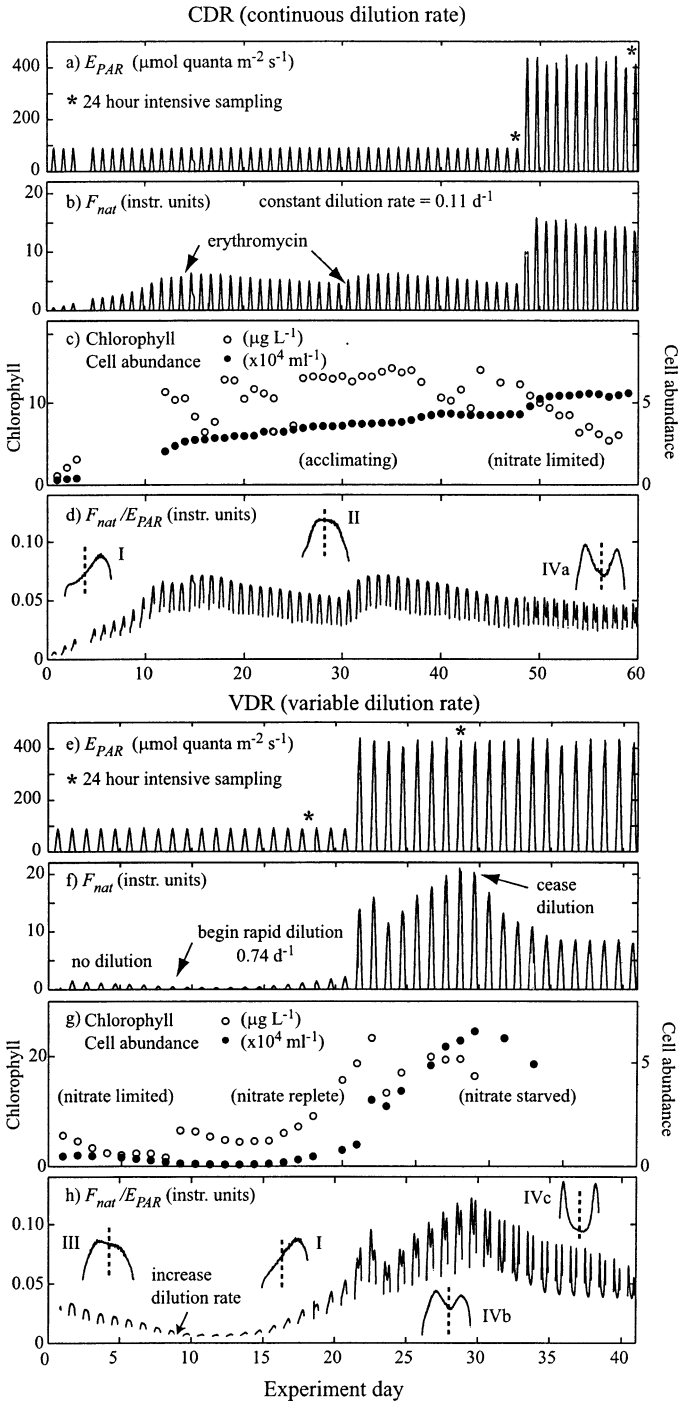

Fig. 1. An overview of the treatments applied to the (a–d) ''constant'' dilution rate (CDR) and (e–h) ''variable'' dilution rate (VDR) cultures. Shifts from low to high E_{PAR} (a, e) occur between two 24-h intensive sampling periods (star symbols). F_{nat} and E_{PAR} data were lost between CDR days 3 and 4 and midday on CDR day 48. Also, resulting changes in (b, f) F_{nat}, (c, g) *chl* and cell abundance, and (d, h) F_{nat}/E_{PAR}. Roman numerals (d, h) indicate specific diurnal patterns referenced in the text; vertical dashed lines on the diurnal patterns indicate solar noon.

AU-10) for redundancy, and in situations when the volume of available sample was insufficient for HPLC analysis.

These cultures were also sampled intensively at ≈90-min intervals twice during each experiment, once just before and once several days after the shift from low to high E_{max} (Fig. 1a,e star symbols: CDR days 47 and 59 and VDR days 17 and 28, respectively). During the CDR experiment, the low dilution rate limited the volume of culture available for analyses. Consequently, only fluorometric *chl* and cell abundance were sampled intensively on days 47 and 59. During the VDR experiment, however, enough sample was available on 90-min intervals to conduct HPLC analyses as well.

Natural fluorescence measurements—A photomultiplier tube and a filter set specific to chlorophyll fluorescence (685-nm center wavelength, 30-nm FWHM, Omega Optical 685WB30) were used to measure the total natural fluorescence at small solid angle. Both this signal (F_{nat}, instrument units) and the scalar irradiance between 400 and 700 nm in the center of the culture vessel (E_{PAR}, μmol quanta m^{-2} s^{-1}) were digitized continuously at 0.25 Hz. From these measurements we computed the ratio F_{nat}/E_{PAR}, a proxy for natural fluorescence yield. This ratio quantified the variability in F_{nat} that could not be ascribed to the direct and instantaneous influence of irradiance. Similar proxies have been used to examine F_{nat} variability in dynamic irradiance environments (e.g., Letelier and Abbott 1996; Cullen et al. 1997; Maritorena et al. 2000). Because F_{nat} and E_{PAR} at low or zero E_{PAR} primarily reflected electronic noise and bias, we removed from the analysis all data corresponding to E_{PAR} conditions less than 2 μmol quanta m^{-2} s^{-1}. Also, because the spectral character of the lamp used in this study varied only negligibly with intensity, we did not add a spectral dimension to F_{nat}/E_{PAR}.

Variable fluorescence measurements—In both experiments, a small volume of culture was continuously circulated through the dark chamber of a Fast Repetition Rate fluorometer (FRRF, Fasttracka, Chelsea Instruments). Circulation of the culture was rapid; only ≈90 s elapsed between removal from ambient light conditions and measurement by the FRRF. Since this time scale is short compared to that of nonphotochemical quenching (NPQ, tens of min), but long compared to the relaxation of photochemical quenching (PQ, ms), we presume that the quenching present in the variable fluorescence kinetics reflects NPQ experienced by the phytoplankton in the culture vessel. FRRF flashlet sequences were binned to 1-min intervals and analyzed using software written by one of the authors (Laney 2003). Instrument biases were characterized and corrected for according to Laney (2003) to produce estimates of (1) the quantum yield of PSII (commonly denoted as F_v/F_m), (2) the functional cross section of PSII (σ_{PSII}), and (3) the reoxidation time constant (τ) of the acceptor side of PSII. The irradiance at which the rate of primary photochemistry equals the rate of electron flow through PSII (E_K) was estimated from σ_{PSII} and τ following Falkowski (1992). This E_K is a photochemical analog of, but is not identical to, the photosynthetic saturation irradiance E_K commonly estimated from primary production incubation experiments.

Field measurements of diurnal kinetics in natural fluorescence—We measured F_{nat} and E_{PAR} within a 30,000-km^2 coastal frontal region in the Gulf of Alaska during a 30-d mesoscale study in May 2003. Irradiance and water-leaving radiance at seven wavelengths, including a 683-nm band for the determination of F_{nat}, were sampled at 6 Hz using a microSAS radiometer (Satlantic). The guidelines of Mueller et al. (2003) were followed to correct for potential artifacts resulting from sun glint and observational geometry. Fluorescence line height (FLH) was computed from the spectral radiances following Letelier and Abbott (1996). These FLH data were normalized for changes in phytoplankton biomass, with estimates of near-surface chlorophyll concentration derived using a nine-wavelength absorption–attenuation spectrophotometer (ac-9, WETLabs) that continuously sampled the ship's uncontaminated seawater supply, drawn from 3 m in depth. Chlorophyll concentration was estimated as the difference between spectral absorption at 676 and 650 nm, divided by 0.014 m^{-1} μg chl^{-1} L. Both absorption wavelengths were corrected for scatter artifacts using absorption at 715 nm. The ac-9 was calibrated daily with optically ''clean'' water, and 0.2-μm filtered seawater was also measured every few hours to provide correction for absorption artifacts due to dissolved material.

Results

Variability in natural fluorescence—The absolute magnitude of F_{nat} in both culture experiments was strongly affected by the instantaneous ambient irradiance intensity (Fig. 1b,f). The daily maximum in F_{nat} occurred at solar noon, when E_{PAR} was most intense. Large increases in F_{nat} occurred coincidentally with each shift from low to high photoperiod E_{max} (CDR day 48 and VDR day 21). However, in neither culture was the increase in F_{nat} directly proportional to E_{max}. In the slowly growing but stable CDR population, the fivefold increase in E_{max} resulted in only a threefold increase in F_{nat}. Over the following 10 d, the daily maximum in F_{nat} decreased in magnitude by ≈10%, during which time *chl* biomass decreased by about 50% (Fig. 1c). In the VDR culture, an identical fivefold increase in E_{max} resulted in a roughly sevenfold increase in F_{nat} in this rapidly growing population. Over the following 10 d, changes in daily maximum F_{nat} roughly followed daily changes in *chl* biomass and cell abundance (Fig. 1g).

During days of low E_{max}, we observed three general diurnal patterns in F_{nat} yield (Fig. 1d,h). During periods of positive population growth, diurnal F_{nat}/E_{PAR} exhibited an increasing and roughly linear trend for the majority of the day (pattern I). When populations were relatively stable, midday F_{nat}/E_{PAR} was diurnally symmetric (pattern II). In decreasing populations, midday F_{nat}/E_{PAR} exhibited a slight decreasing trend around solar noon (pattern III). Transitions between one pattern and another were in some instances gradual, when the CDR culture changed slowly from I to II as those cells acclimated to low nitrate availability between CDR days 0 and 15. At other times, these patterns changed suddenly, such as on VDR days 8–9, during which a switch from pattern III to I occurred within 24 h following a step increase in media dilution rate.

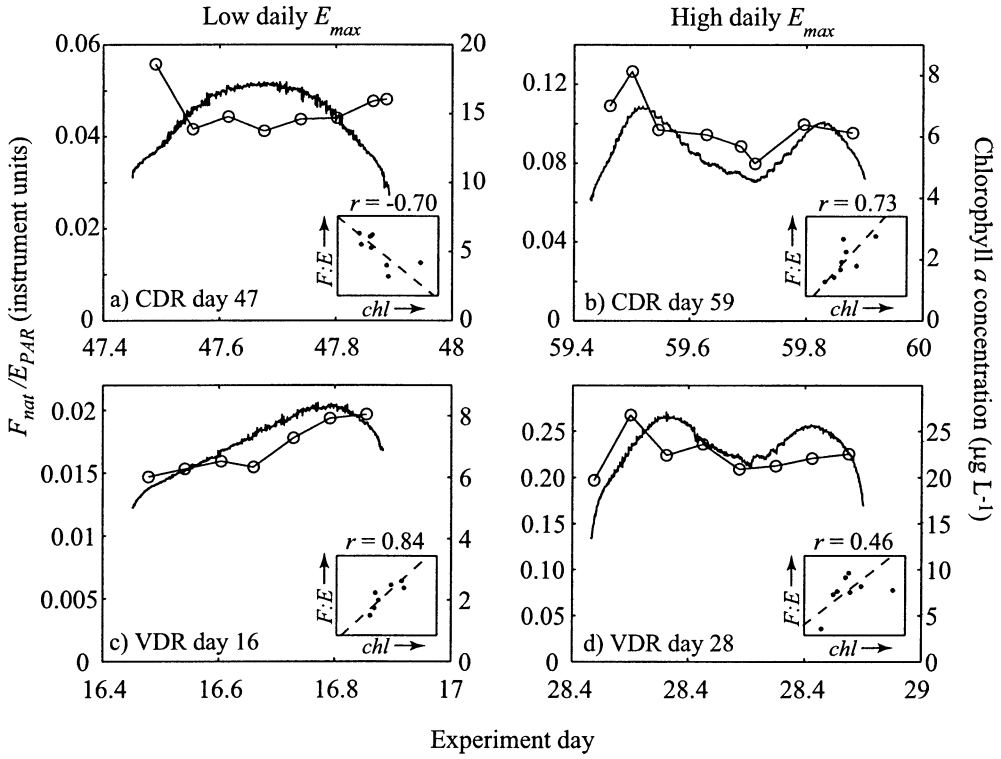

Fig. 2. The diurnal relationship between F_{nat}/E_{PAR} (continuous lines) and chlorophyll biomass (joined circles) for the four intensive discrete sampling periods. Insets show the corresponding scatter plots of F_{nat}/E_{PAR} and *chl*, with the corresponding Model II linear geometric mean regressions (dashed lines) and correlation coefficients *r*.

Under high daily E_{max} conditions, substantial quenching of F_{nat} was evident around solar noon in both the CDR and VDR cultures. Such quenching led to characteristic midday depressions in F_{nat}/E_{PAR}. These depressions were more pronounced in the slowly diluted CDR culture (pattern IVa) than in the rapidly diluted portion of the VDR culture (pattern IVb). The midday depression deepened considerably and progressively in the VDR culture following cessation of dilution on VDR day 29 (pattern IVc). Midday depressions similar to those observed in the F_{nat}/E_{PAR} data also occurred in diurnal time series of F_v/F_m, immediately following the shift from low to high E_{max} (data not shown).

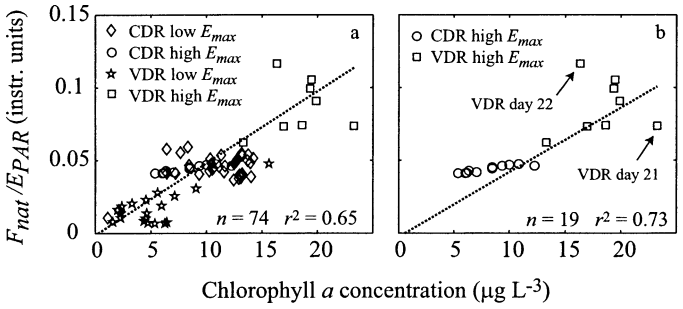

Fig. 3. The relationship between *chl* and noontime F_{nat}/E_{PAR} comprising (a) pooled data from all days in both cultures and (b) only those days corresponding to high E_{max} light treatments. Dashed lines indicate a Model II linear regression (geometric mean method). Arrows (b) denote points corresponding to the first 2 d following the increase in E_{max} in the VDR culture.

Intensive 24-h sampling indicated that diurnal changes in *chl* biomass could not account for the observed diurnal patterns in F_{nat}/E_{PAR}. Functional relationships between these nondependent variables were determined using Model II regression methods (Laws and Archie 1981; Laws 1997). The overall correlation between F_{nat}/E_{PAR} and *chl* within each of these four intensive sampling periods differed not only in proportion but also in sign (Fig. 2, insets). Changes in *chl* and F_{nat}/E_{PAR} were positively correlated in only three of these four intensive sampling periods. The correlation was strongest in the VDR culture under low E_{max} conditions (Fig. 2c) and weakest in the VDR culture under high E_{max} conditions (Fig. 2d). A strong negative relationship between *chl* and F_{nat}/E_{PAR} was observed in the CDR culture under low E_{max} conditions (Fig. 2a). Because we do not assume that changes in F_{nat} are driven by *chl* over all temporal scales, negative or poor correlations between these two variables are acceptable.

Long-term variability in F_{nat}/E_{PAR}—Over longer time scales of days to weeks, the daily chlorophyll biomass measurements in these cultures were correlated positively but not strongly with noontime F_{nat}/E_{PAR} (Fig. 3a, $r^2 = 0.65$, $n = 74$, geometric mean Model II regression). This correlation improved slightly when considering only those days with high E_{max}, presumably as being more representative of remotely sampled F_{nat} data (Fig. 3b, $r^2 = 0.73$, $n = 19$). This

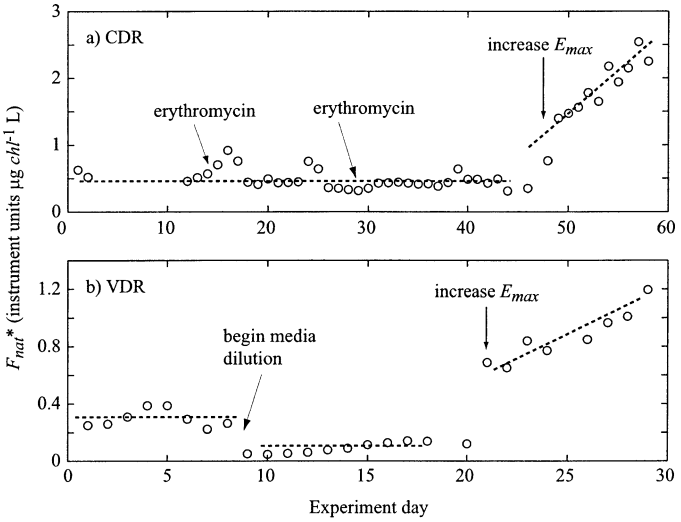

Fig. 4. Long-term changes in F^*_{nat} (the ratio of noon F_{nat} to predawn *chl* biomass) in the (a) CDR and (b) VDR cultures. Dashed lines denote general trends, not statistical fits.

apparently strong correlation only reflects a difference in the F_{nat} versus *chl* relationship between these two cultures; there was little correlation between these variables within each culture when considered separately. The greatest outliers (arrows) corresponded to the 2 d in the VDR culture immediately after the increase in E_{max}. These correlations neither improved nor weakened materially when F_{nat} data sampled at times other than solar noon were used (data not shown).

Long-term kinetics in the ratio of natural fluorescence to chlorophyll—Remote sensing fields of F_{nat} may encompass large gradients in phytoplankton biomass, and normalizing F_{nat} to *chl* biomass is one way to compare F_{nat} kinetics across such large dynamic ranges. We normalized F_{nat} sampled at solar noon for all days by the daily *chl* measurement to form a daily index of chlorophyll-normalized F^*_{nat}, with notation analogous to that of a^* (Fig. 4). The magnitude of this index under low E_{max} conditions in the CDR culture was roughly comparable to the initial, low-nitrate phase of the VDR culture. In each instance cells were acclimating to very low levels of available nitrate. Only the first of the dilute erythromycin additions to the CDR culture corresponded with a weak increase in F^*_{nat} over a 5-d period. Increasing the dilution rate on VDR day 9 in the VDR culture resulted in an immediate and substantial decrease in F^*_{nat}, which rebounded to approximately half of its predilution level over the following nine generations. The shift up in E_{max} in both cultures resulted in increases in F^*_{nat} far exceeding any transient observed under low E_{max} conditions. During the days following each increase in E_{max}, F^*_{nat} increased in a roughly linear fashion as cells acclimated to high light conditions. Day-to-day increases in F^*_{nat} under high E_{max} conditions were more rapid in the CDR culture than in the VDR culture.

Diurnal natural fluorescence kinetics—The midday F_{nat} kinetics under high light conditions (e.g., patterns IVa–c) in Fig. 1) are difficult to parameterize when plotted as a function of time. However, these patterns condensed into a single family of curves when plotted as a function of ambient irradiance (Fig. 5a–c). Between dawn and solar noon, F^*_{nat} increased in a roughly linear fashion with E_{PAR}, up to a certain threshold irradiance (vertical dashed lines). Slight deviations from linearity can be observed in some cases (arrows, Fig. 5a,b). Above this threshold irradiance the relationship between F^*_{nat} and E_{PAR} was considerably reduced in magnitude. Afternoon changes in F^*_{nat} as ambient intensity decreased were roughly the reverse of those in the morning, except for a small degree of hysteresis that caused afternoon F^*_{nat} to be consistently lower than that at equivalent irradiances in the morning (Fig. 5a–c, dotted traces). When F^*_{nat} is normalized by the instantaneous irradiance, two distinct regions of fluorescence quenching can be distinguished, falling above and below the threshold irradiance (Fig. 5d–f). We interpret these two regions of F^*_{nat} quenching to reflect photochemical and nonphotochemical processes, respectively. The threshold irradiance separating the two regions was not found to be associated universally with diurnal trends in any one of the variable fluorescence parameters F_v/F_m, σ_{PSII}, τ, or with the E_K computed from σ_{PSII} and τ (Fig. 5g–u). However, the irradiance at which the F_{nat} versus E_{PAR} relationship changed (Fig. 5a–c, vertical dashed lines) generally coincided with the irradiance at which E_{PAR} exceeded the computed photochemical E_K (Fig. 5g–i).

We developed a simple three-parameter model to describe these diurnal F_{nat} kinetics and used a numerical fitting procedure to quantify day-to-day changes in these parameters (Fig. 6). This approach characterizes diurnal F_{nat} kinetics in terms of the threshold irradiance E_{thresh} at which changes in quenching occur and the slope of the F_{nat} versus E_{PAR} relationship at irradiances below and above this point. For an initial assessment of long-term changes in these kinetics, we considered only F_{nat} kinetics before solar noon. Consequently, this parameterization does not include terms to describe the hysteresis effect observed in afternoon F_{nat} yield.

Using this parameterization, we found that the relationship between F_{nat} and E_{PAR} at irradiances below the threshold increased during the days following the shift up in E_{max} in both cultures (Fig. 6a,b; open symbols). The absolute magnitudes were different, however, with the nitrate-limited CDR culture always emitting more fluorescence per unit E_{PAR} and *chl* than the nitrate-replete VDR culture. Similar day-to-day trends were observed in the relationship between F_{nat} and E_{PAR} after the diurnal onset of fluorescence quenching (closed symbols). Again, the CDR culture exhibited a greater F_{nat} yield at high irradiances per unit *chl* than the comparatively nitrate-replete VDR culture did. Such smoothly varying, monotonic responses were not observed in these parameters during a period of nitrate starvation later in the VDR culture (Fig. 6c).

The percent difference in the F_{nat} versus E_{PAR} relationship below and above E_{thresh} varied little in the CDR culture after its shift to high E_{max} conditions (Fig. 6d). For the VDR culture, however, this percentage increased steadily after the shift to high E_{max}, indicating an increase in the relative magnitude of midday F_{nat} quenching over this period (Fig. 6e). When media dilution later ceased, this trend reversed and

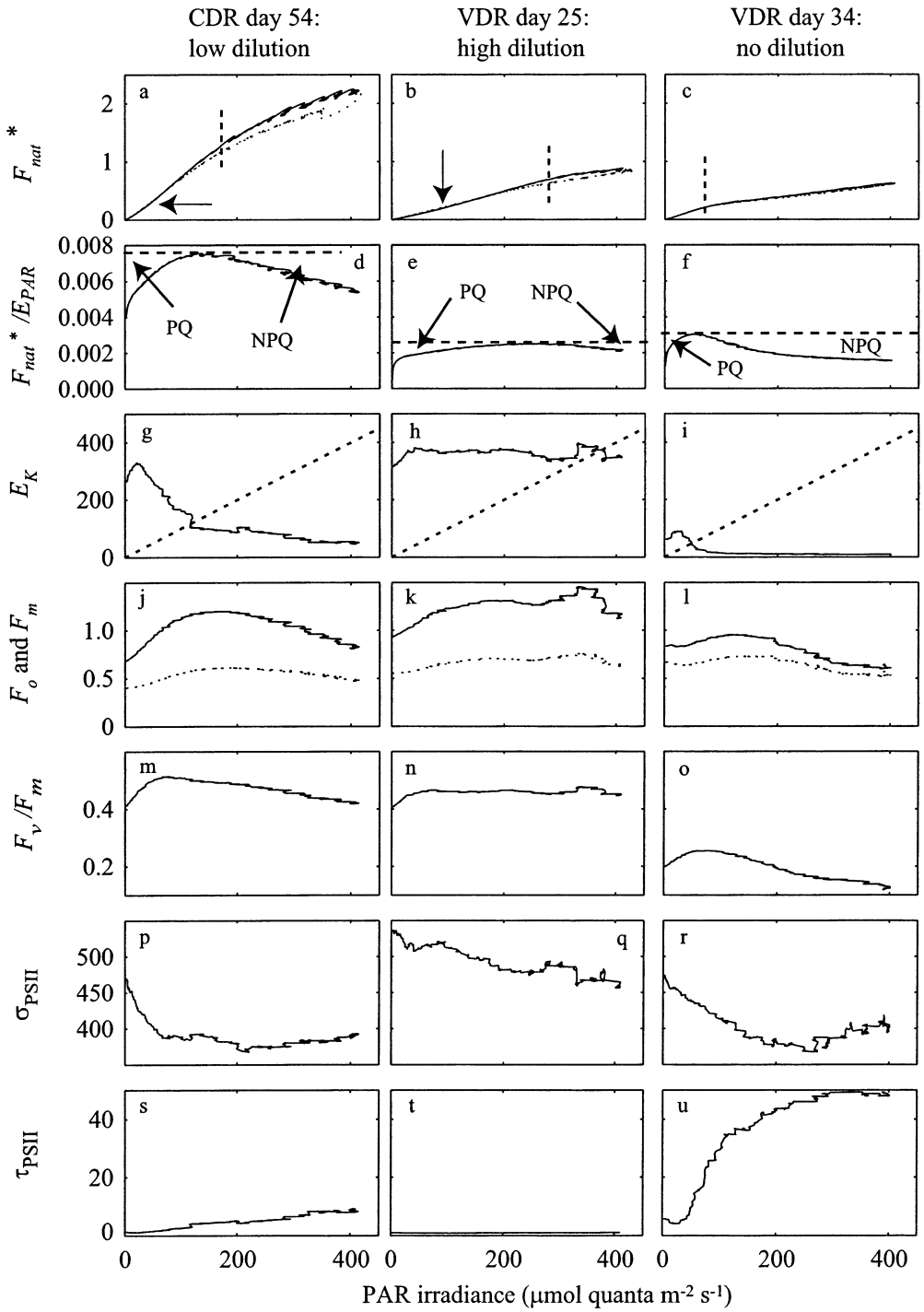

Fig. 5. Concomitant changes for three characteristic days of these experiments in (a–c) F_{nat}^* F_{nat} per unit chlorophyll in relative units, (d–f) F_{nat}^*/E_{PAR}, (g–i) the photochemical E_K in μmol quanta m^{-2} s^{-1}, computed from σ_{PSII} and τ, and (j–u) variable fluorescence parameters F_o and F_m, F_v/F_m, σ_{PSII} in Å^2 RCII^{-1} quanta^{-1}, and τ in ms. For F_{nat}, solid lines represent measurements before solar noon, dotted traces indicate afternoon measurements, vertical dashed lines indicate the approximate location of the onset of nonphotochemical quenching, and arrows refer to features discussed in the text. In (d–f), ''PQ'' indicates regions in which photochemical processes dominate quenching of F_{nat}, and ''NPQ'' indicates regions in which nonphotochemical processes dominate. Dashed lines (g–i) indicate a 1 : 1 relationship between E_K and E_{PAR}. In (c) and (f), discrete chlorophyll data were not available for VDR day 34, and a correlation between F_m and *chl* was used to scale F_{nat} measurements into F_{nat}^*.

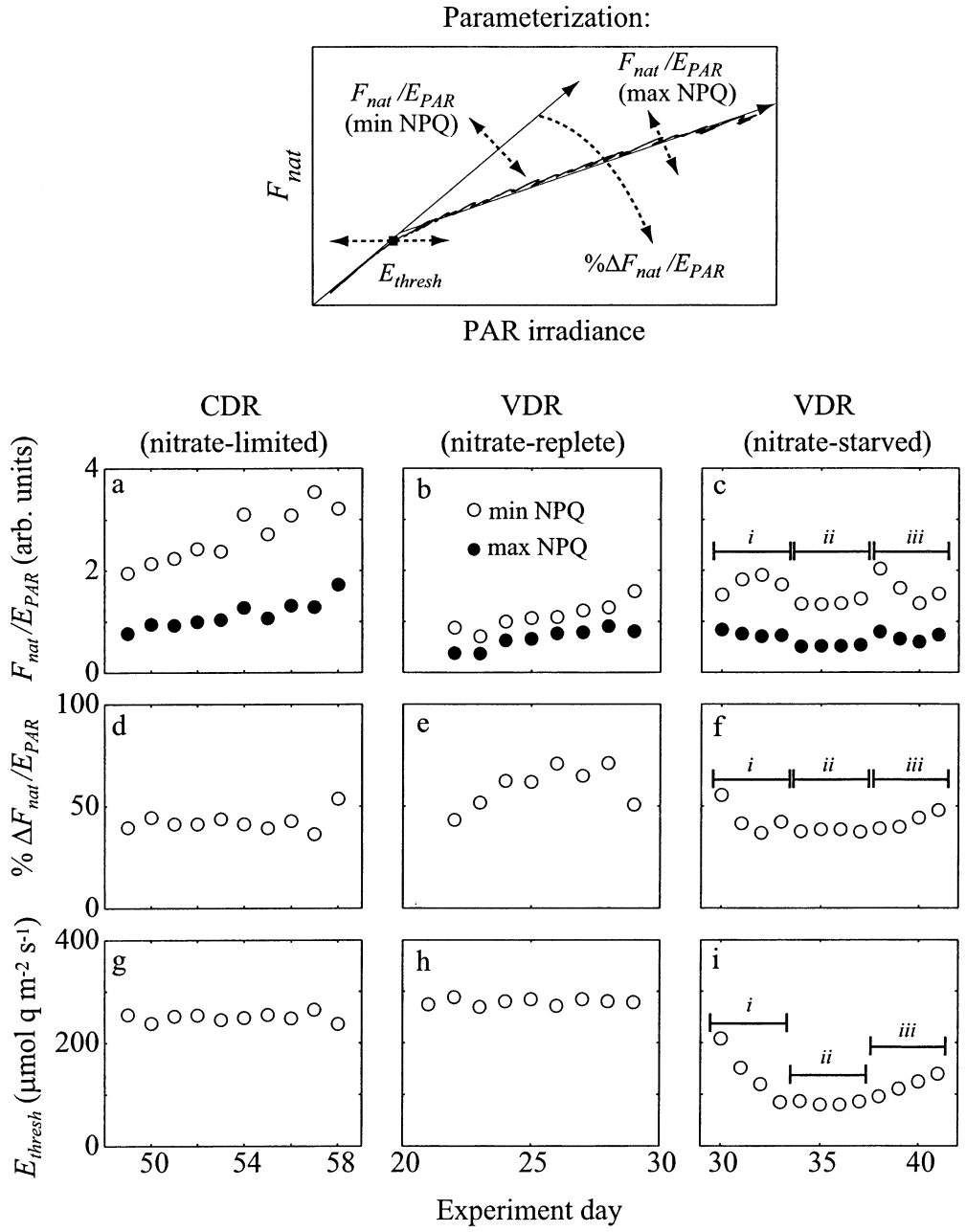

Fig. 6. The parameterization used to quantify the empirical parameters from morning F_{nat} kinetics. Also, changes in these parameters that occur for the (a, d, g) CDR nitrate-limited; (b, e, h) VDR nitrate-replete; and (c, f, i) VDR nitrate-starved phases of these cultures. The percent difference in F_{nat}/E_{PAR} (d–f) is calculated as the ratio of max to min NPQ. Three distinct responses in the nutrient-starved phase of VDR are indicated by small Roman numerals (*i–iii*).

restored within 3 d to low values comparable to those seen earlier in the VDR culture (Fig. 6f).

The threshold irradiance E_{thresh} that characterizes the change in F_{nat} quenching was about 10% higher in the VDR than in the CDR culture (Fig. 6g,h), but this parameter showed little day-to-day variability when dilution rates were steady. However, E_{thresh} decreased dramatically in the VDR culture from ≈210 to ≈80 μmol quanta m^{-2} s^{-1} in the period of nitrate starvation following the cessation of media dilution on VDR day 29. Three phases in E_{thresh} were observed in the remaining 12 d of the VDR culture: a rapid linear decrease for 4 d, a stable period for 4 d, and a slow rise for the final 4 d (Fig. 6i, *i—iii*). Boundaries between these three phases coincide with observed fluctuations in the other F_{nat} parameters (Fig. 6c,f).

Discussion

Systematic long-term trends in the parameters used to characterize subdiurnal kinetics in F_{nat} yield confirm that

these kinetics contain information about the photosynthetic state of these cultures and their responses to environmental manipulation. In order to interpret the evolution of these parameters, we first consider their probable physiological bases. Next we compare the F_{nat} kinetics observed in these cultures to those measured in natural phytoplankton assemblages. Finally, we discuss how certain aspects of these kinetics may affect the interpretation of variability in fields of remotely sensed F_{nat}.

Natural fluorescence kinetics in T. weissflogii—The most prominent diurnal feature in F_{nat} yield displayed by this model diatom was a distinct midmorning increase in quenching above the threshold irradiance E_{thresh}. This feature most likely reflects an increase in nonphotochemical quenching resulting from the conversion of the photosynthetic accessory xanthophyll diatoxanthin (DD) into the photoprotective xanthophyll diadinoxanthin (DT). Interconvertible xanthophylls provide a mechanism for energy dissipation both in diatoms and in other phytoplankton species (Lavaud et al. 2004). An increase in the relative proportion of diadinoxanthin thermally dissipates more absorbed light energy and decreases the fraction of excitation arriving at the easily damaged PSII reaction centers (Müller at al. 2001), thus decreasing the level of fluorescence. Xanthophyll interconversion is thought to be triggered by the strength of the trans-thylakoid proton gradient; DD converts to DT when the proton concentration in the lumen exceeds that in the stroma by some threshold level (Demmig-Adams and Adams 1992). Since this gradient is established by primary photochemistry in PSII, changes in E_{thresh} over time scales longer than a photoperiod should be largely independent of population level responses in cell abundance or chlorophyll biomass.

Instead, long-term changes in E_{thresh} may more likely reflect physiological changes related to processes that affect maximal photosynthetic rate. The level of excitation pressure on PSII reaction centers at any given instant can be qualitatively assessed by comparing E_{PAR} to E_K (Falkowski 1992). When E_{PAR} surpasses E_K, absorbed light energy is delivered to the photosynthetic electron transport chain at a rate exceeding its maximal throughput rate. Under nutrient-limited or nutrient-starved conditions in these cultures, E_{thresh} values usually exceeded the level at which E_{PAR} surpassed E_K, indicating that photosynthetic electron transport operated at maximal levels prior to DD–DT interconversion (Fig. 5g–i). In contrast, E_{thresh} in nutrient-replete conditions occurred at irradiances lower than those at which E_{PAR} surpassed E_K, indicating that DD–DT interconversion occurred prior to photosynthetic electron transport rates being maximal. A concern with this assessment is that the photochemical E_K was computed directly from σ_{PSII} and τ, which were determined using a variable fluorometer with a spectrally narrow excitation source. These E_K will be unavoidably biased if the measured σ_{PSII} and τ differ considerably from analogous parameters determined using a spectrally broader excitation source more representative of the ambient irradiance.

Photochemical quenching of F_{nat} also appears to be evident in the diurnal F_{nat} yield kinetics of these cultures at irradiances below E_{thresh} (Fig. 5d–f). The integrated areas above the F_{nat} yield curve and below the maximum F_{nat} yield attained show the relative influence of photochemical and nonphotochemical quenching processes on F_{nat} yield. Photochemical quenching processes presumably drive the decreases in F_{nat} yield from maximal at irradiances less than E_{thresh}, whereas nonphotochemical processes drive the decreases in F_{nat} yield observed at irradiances greater than E_{thresh}. Given this interpretation, the data presented in Fig. 5d–f would indicate that PQ is greater in this model diatom when nitrate is readily available than when nitrate is scarce. Also, NPQ is greater when nitrate is scarce than when it is readily available.

Unlike the shape of these diurnal F_{nat} kinetics, the absolute magnitude of the F_{nat} versus E_{PAR} relationship is very sensitive to changes in chlorophyll biomass. As a result, long-term trends in the actual value of F_{nat}/E_{PAR} will be influenced by long-term changes in chlorophyll biomass. In general, the magnitudes of F_{nat}/E_{PAR} below and above E_{thresh} covaried in these two cultures (Fig. 6a–c), except under nitrate-starvation conditions at the end of the VDR culture, when these two parameters became decoupled over a period of 3–4 d. This observation indicates that physiological changes in energy distribution in the photosystem related to the xanthophyll cycle may not be an important consideration for using F_{nat} to estimate *chl*, except, potentially, under conditions of changing nitrate availability.

The percent increase in F_{nat} quenching above E_{thresh} ($\%\Delta F_{nat}/E_{PAR}$) also differed in these cultures depending on nitrate availability. Natural fluorescence was less strongly quenched when nitrate was replete in the VDR culture than when it was scarce in either the VDR or CDR cultures (Fig. 6d–f). If the physiological basis for changes in F_{nat}/E_{PAR} at the threshold irradiance is the conversion of diatoxanthin into diadinoxanthin, the magnitude of $\Delta F_{nat}/E_{PAR}$ in these cultures should scale with their nonphotochemical capacity to quench F_{nat}. However, the volume of sample available daily in the CDR culture was inadequate to assess diel variability in the interconvertible xanthophylls. The daily pigment data showed no conclusive correlation between these xanthophylls and the degree of nonphotochemical quenching above the threshold irradiance (data not shown).

Natural fluorescence kinetics in field populations—We observed diurnal F_{nat} kinetics similar to those expressed by our diatom cultures in a summer neritic phytoplankton assemblage, but only after substantial averaging (Fig. 7). The threshold irradiance in these assemblages occurred at approximately 200 μmol quanta m^{-2} s^{-1}. The similarity between these diurnal F_{nat} kinetics and those of our cultures is encouraging and indicates that the parameterization we developed for the diatom cultures (i.e., Fig. 6) may be appropriate for at least some natural phytoplankton assemblages.

Taxonomic differences in photosynthetic physiology can strongly affect F_{nat} kinetics, and so our parameterization may not be appropriate for characterizing diurnal F_{nat} kinetics in all assemblages (e.g., in oligotrophic regions dominated by picoeukaryotes or prokaryotes). Consequently, when assessing F_{nat} variability in natural assemblages, it is essential to select an appropriate parameterization for diurnal F_{nat} kinetics. We developed such a parameterization empirically, but other studies have employed analytical functions to describe

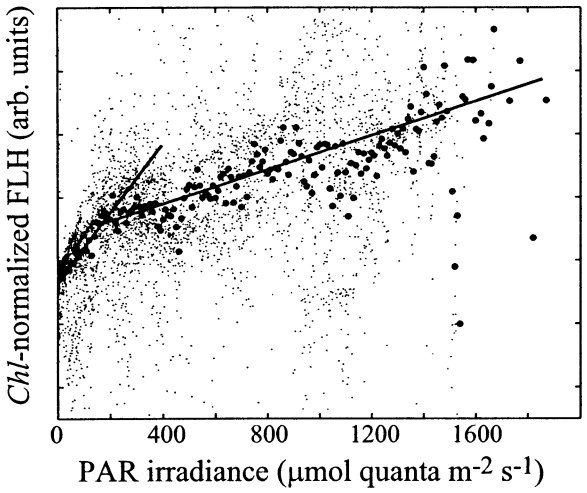

Fig. 7. Water-leaving FLH, normalized for *chl* (small points), as a function of incident solar irradiance for 30 d of continuous observation in the Gulf of Alaska. Closed circles represent these data binned on 10 μmol quanta m^{-2} s^{-1} intervals. Lines represent general trends.

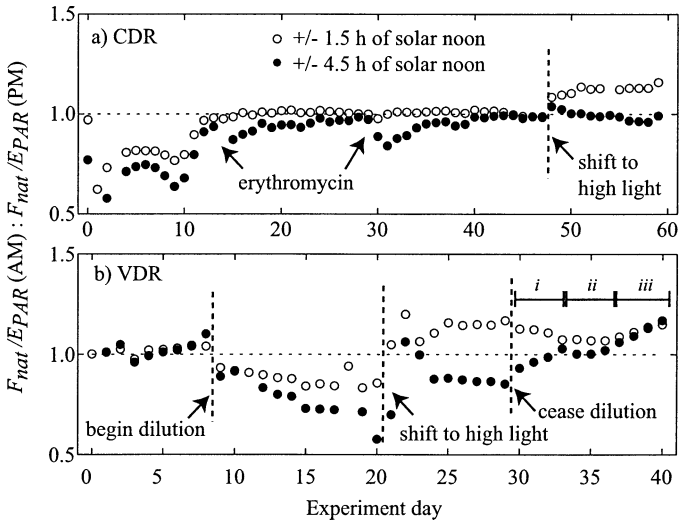

Fig. 8. Daily changes in the ratio of morning to afternoon F_{nat}/E_{PAR} for the (a) CDR and (b) VDR cultures. Results from two different sampling intervals are indicated by closed (±4.5 h around solar noon) and open symbols (±1.5 h around solar noon).

the relationship between F_{nat} and E_{PAR}. For example, Schallenberg et al. (2002) used a saturating exponential equation with Bering Sea assemblages. Such a parameterization requires that F_{nat} plateau at high irradiances, a behavior not observed in our diatom cultures nor in our field measurements. On closer examination, the Bering Sea F_{nat} data also do not appear to plateau with increasing E_{PAR}, but instead continue to increase, albeit with a reduced slope.

Similarly, a linear parameterization was used by Letelier et al. (1997) to relate F_{nat} and irradiance under low light conditions in Southern Ocean assemblages. Our results indicate that the first-order behavior of diurnal F_{nat} kinetics is in fact roughly linear at low irradiances. However, at higher irradiances, the diurnal behavior of F_{nat} in those Southern Ocean data appears to resemble more closely the empirical parameterization we present here. Lacking a universally applicable deterministic model for variability in F_{nat}, it is impossible to know a priori what specific analytical parameterization to use when examining natural assemblages. For any initial assessment or quantification of long-term variability in diurnal F_{nat} kinetics, an empirical parameterization may be less susceptible to artifacts that result from selection of an inappropriate analytical function.

Remote sensing considerations—Our results support prior studies in the sense that changes in F_{nat} or F_{nat} yield can correlate reasonably well with changes in *chl* over large dynamic ranges (Fig. 3). However, our results demonstrate the degree to which environmental factors can alter the relationship between F_{nat} and *chl* (Fig. 4). Ultimately, the sensitivity with which remote sensors can resolve changes in *chl* or any other variable of interest from F_{nat} depends on the physiological relationship between these variables, not on the radiometric sensitivity of the sensor. Subdiurnal variability in the relationship between F_{nat} and *chl* was considerable in these cultures (Fig. 2) and could introduce error or bias into remotely sensed estimates of *chl* derived from F_{nat}.

Weaknesses in the correlation between F_{nat} and *chl* indicate situations in which F_{nat} may provide insight into photosynthetic variability. Daily sampling of F_{nat} may be sufficient for identifying broad photosynthetic responses (e.g., Fig. 4), but additional and possibly more ecologically meaningful interpretations require better sampling on subdiurnal scales. Autonomous aircraft or geostationary satellites such as the Hyperspectral Environmental Suite on the next generation of GOES satellites could in theory provide the time series of F_{nat} that would be necessary for resolving subdiurnal kinetics in both F_{nat} and biomass. This, in turn, might allow physiological parameters such as E_{thresh} to be directly measured by a single remote sensor.

Current satellite sensors individually do not provide effective multiple sampling in a single day, but one way to increase the effective sampling frequency is to combine data collected from separate sensors. We modeled how the MODIS sensors sampling at different times of the day onboard the Terra and Aqua satellites might perceive the diurnal F_{nat} variability expressed by our model diatom cultures. We simulated the daily flyovers of Terra and Aqua by subsampling our laboratory F_{nat}/E_{PAR} time series twice daily, 1.5 h before solar noon (Terra) and 1.5 h after (Aqua). For each diurnal pair of samples we calculated the ratio of forenoon to afternoon F_{nat}/E_{PAR} for the entirety of both cultures (Fig. 8). Time series of this AM : PM ratio under low E_{max} conditions exhibited features that related qualitatively to trends in nitrate availability and population growth in the cultures (open circles). Environmental disturbances, such as changes to the media dilution rate, can be clearly seen in this AM : PM ratio, as were both erythromycin additions. By comparison, an index generated from single daily sampling of F_{nat} did not clearly indicate the second of these additions (Fig. 4a). Fluctuations in this AM : PM ratio in the period after dilution ceased on VDR day 29 (Fig. 8b, open circles) corresponded

with the three phases, *i–iii*, observed in our three diurnal F_{nat} parameters (Fig. 6c,i).

We also computed this AM : PM ratio using a wider sampling interval of ±4.5 h that would be less affected by the strong midday quenching of F_{nat}. We note that changing the sampling interval clearly has considerable effect on the long-term behavior of this type of index (Fig. 8a,b; closed circles). With preliminary findings from a single diatom species, it is difficult to identify the interval that would produce the most robust AM : PM ratio. A large database of F_{nat} yield measured in natural assemblages would be very helpful and would provide valuable information about the actual F_{nat} kinetics expressed by surface ocean assemblages. Such a climatology has not yet been assembled, but parameters like F_{nat}/E_{PAR} may be useful in this respect because both F_{nat} and E_{PAR} are easily measured using simple radiometric sensors. Successful autonomous sampling of F_{nat} and E_{PAR} in situ using moorings and drifters has been demonstrated already over large spatial and temporal scales (e.g., Abbott and Letelier 1997*a,b*; Abbott et al. 2000, 2001). A more detailed understanding of the actual diurnal variability in F_{nat} in natural assemblages is essential for improving our ability to interpret variability in remotely sensed F_{nat} from current or future satellite sensors.

References

ABBOTT, M. R., AND R. M. LETELIER. 1997*a*. Bio-optical drifters—scales of variability of chlorophyll and fluorescence. Soc. Photo-Optical Instrument. Engineers **2963:** 216–221.

———, AND ———. 1997*b*. Going with the flow—the use of optical drifters to study phytoplankton kinetics, p. 143–168. *In* M. Kahru and C. W. Brown [eds.], Monitoring algal blooms: New techniques for detecting large-scale environmental changes. Landes.

———, J. G. RICHMAN, R. M. LETELIER, AND J. S. BARTLETT. 2000. The spring bloom in the Antarctic Polar Frontal Zone as observed from a mesoscale array of bio-optical sensors. Deep-Sea Res. II **47:** 3285–3314.

———, ———, J. S. NAHORNIAK, AND B. S. BARKSDALE. 2001. Meanders in the Antarctic Polar Frontal Zone and their impact on phytoplankton. Deep-Sea Res. II **48:** 3891–3912.

BABIN, M., A. MOREL, AND B. GENTILI. 1996. Remote sensing of sea surface sun-induced chlorophyll fluorescence: Consequences of natural variations in the optical characteristics of phytoplankton and the quantum yield of chlorophyll *a* fluorescence. Int. J. Remote Sensing **17:** 2417–2448.

BORSTAD, G. A., H. R. EDEL, J. F. R. GOWER, AND A. B. HOLLINGER. 1985. Analysis of test and flight data from the Fluorescence Line Imager. Can. Spec. Pub. Fish. Aquat. Sci. **83:** 1–46.

CAMPBELL, D., V. HURRY, A. K. CLARKE, P. GUSTAFSSON, AND G. ÖQUIST. 1998. Chlorophyll fluorescence analysis of cyanobacterial photosynthesis and acclimation. Microb. Molec. Biol. Rev. **62:** 667–683.

CHEKALYUK, A. M., AND M. YU GORBUNOV. 1994. Diel variability of in vivo fluorescence in near-surface water layer, p. 140–151. *In* J. S. Jaffee [ed.], Ocean Optics XII. Proc. SPIE 2258.

CULLEN, J. J., A. M. CIOTTI, R. F. DAVIS, AND P. J. NEALE. 1997. The relationship between near-surface chlorophyll and solar-stimulated fluorescence: Biological effects, p. 272–277. *In* S. G. Ackleson and R. Frouin [eds.], Ocean Optics XIII. Proc. SPIE 2963.

———, AND M. R. LEWIS. 1995. Biological processes and optical measurements near the sea surface: Some issues relevant to remote sensing. J. Geophys. Res. **100:** 13255–13266.

DEMMIG-ADAMS, B., AND W. W. ADAMS III. 1992. Photoprotection and other responses of plants to high light stress. Ann. Rev. Plant. Phys. Plant. Mol. Biol. **43:** 599–626.

ESAIAS, W. E., AND OTHERS. 1998. An overview of MODIS capabilities for ocean science observations. IEEE Trans. Geo. Rem. Sens. **36:** 1250–1265.

FALKOWSKI, P. G. 1992. Molecular ecology of phytoplankton photosynthesis, p. 47–68. *In* P. G. Falkowski and A. D. Woodhead [eds.], Primary productivity and biogeochemical cycles in the sea. Plenum.

———, AND Z. KOLBER. 1995. Variations in chlorophyll fluorescence yields in phytoplankton in the world oceans. Aust. J. Plant Physiol. **22:** 341–355.

GARCIA-MENDOZA, E., AND H. MASKE. 1996. The relationship of solar-stimulated natural fluorescence and primary productivity in Mexican Pacific waters. Limnol. Oceanogr. **41:** 1697–1710.

GOWER, J. F. R., AND G. BORSTAD. 1981. Use of the in-vivo fluorescence line at 685 nm for remote sensing surveys of surface chlorophyll *a*, p. 329–338. *In* J. F. R. Gower [ed.], Oceanography from space. Plenum.

HARRIS, D. C., AND M. D. BERTOLUCCI. 1978. Symmetry and spectroscopy: An introduction to vibrational and electronic spectroscopy. Oxford Univ. Press.

HOGE, F. E., P. E. LYON, R. N. SWIFT, J. K. YUNGEL, M. R. ABBOTT, R. M. LETELIER, AND W. E. ESAIAS. 2003. Validation of Terra-MODIS phytoplankton chlorophyll fluorescence line height. I. Initial airborne Lidar results. Appl. Optics **42:** 2761–2771.

IOCCG. 1999. Status and plans for satellite ocean-colour missions: Considerations for complementary missions. J. A. Yoder [ed.], Reports of the International Ocean-Colour Coordinating Group, No. 2, IOCCG.

KIEFER, D. A., W. S. CHAMBERLIN, AND C. R. BOOTH. 1989. Natural fluorescence of chlorophyll *a*: Relationship to photosynthesis and chlorophyll concentration in the western South Pacific gyre. Limnol. Oceanogr. **34:** 868–881.

LANEY, S. R. 2003. Assessing the error in photosynthetic properties determined by fast repetition rate fluorometry. Limnol. Oceanogr. **48:** 2234–2242.

———, R. M. LETELIER, R. A. DESIDERIO, M. R. ABBOTT, D. A. KIEFER, AND C. R. BOOTH. 2001. Measuring the natural fluorescence of phytoplankton cultures. J. Atmos. Ocean. Technol. **18:** 1924–1934.

LAVAUD, J., B. ROUSSEAU, AND A.-L. ETIENNE. 2004. General features of photoprotection by energy dissipation in planktonic diatoms (Bacillariophyceae). J. Phycol. **40:** 130–137.

LAWS, E. 1997. Mathematical methods for oceanographers: An introduction. Wiley.

LAWS, E. A., AND J. W. ARCHIE. 1981. Appropriate use of regression analysis in marine biology. Mar. Biol. **65:** 13–16.

LETELIER, R. M., AND M. R. ABBOTT. 1996. An analysis of chlorophyll fluorescence algorithms for the Moderate Resolution Imaging Spectrometer (MODIS). Remote Sens. Environ. **58:** 215–223.

———, ———, AND D. M. KARL. 1997. Chlorophyll natural fluorescence response to upwelling events in the Southern Ocean. Geophys. Res. Lett. **24:** 409–412.

———, D. M. KARL, M. R. ABBOTT, P. FLAMENT, M. FREILICH, R. LUKAS, AND T. STRUB. 2000. Role of late winter mesoscale events in the biogeochemical variability of the upper water column of the North Pacific Subtropical Gyre. J. Geophys. Res. (C Oceans) **105:** 28723–28739.

MACINTYRE, H. L., T. M. KANA, T. ANNING, AND R. J. GEIDER. 2002. Photoacclimation of photosynthesis irradiance response

curves and photosynthetic pigments in microalgae and cyanobacteria. J. Phycol. **38:** 17–38.

MARITORENA, S., A. MOREL, AND B. GENTILI. 2000. Determination of the fluorescence quantum yield by oceanic phytoplankton in their natural habitat. Appl. Optics **39:** 6725–6737.

MORRISON, J. R. 2003. In situ determination of the quantum yield of phytoplankton chlorophyll *a* fluorescence: A simple algorithm, observations, and a model. Limnol. Oceanogr. **48:** 618–631.

MUELLER, J. L., G. S. FARGION, AND C. R. MCCLAIN. 2003. Ocean optics protocols for satellite ocean color sensor validation, Rev. 4, V III. NASA Technical Manual NASA/TM-2003-21621/ Rev, V III.

MÜLLER, P., X.-P. LI, AND K. K. NIYOGI. 2001. Non-photochemical quenching. A response to excess light energy. Plant Physiol. **125:** 1558–1566.

NEVILLE, R. A., AND J. F. R. GOWER. 1977. Passive remote sensing of phytoplankton via chlorophyll *a* fluorescence. J. Geophys. Res. **82:** 3487–3493.

SARCINA, M., M. J. TOBIN, AND C. W. MULLINEAUX. 2001. Diffusion of phycobilisomes on the thylakoid membrane of the cyanobacterium *Synechococcus* 7942. J. Biol. Chem. **276:** 46830–46834.

SCHALLENBERG, C., M. R. LEWIS, D. E. KELLEY, AND J. J. CULLEN. 2002. ''Variability in the quantum yield of sun-induced fluorescence in the Bering Sea: Effects of light and nutrients.'' *In* Proceedings of *Ocean Optics XVI,* November 18–22, 2002, Santa Fe, New Mexico. SPIE.

SKOOG, D. A., F. J. HOLLER, AND T. A. NIEMAN. 1998. Principles of instrumental analysis. Harcourt Brace.

STEGMANN, P. M., M. R. LEWIS, C. O. DAVIS, AND J. J. CULLEN. 1992. Primary production estimates from recordings of solar-stimulated fluorescence in the equatorial Pacific at 150 degrees west. J. Geophys. Res. **97C:** 627–638.

WRIGHT, S. W., R. F. C. MANTOURA, AND S. W. JEFFREY. 1997. Phytoplankton pigments in oceanography: Guidelines to modern methods. UNESCO.

Received: 10 November 2004
Amended: 30 May 2005
Accepted: 31 May 2005